

## Enhancement in ferroelectricity in V-doped ZnO thin film grown using laser ablation

Tara Dhakal, Devajyoti Mukherjee, Robert Hyde, Hariharan Srikanth, Pritish Mukherjee and Sarath Witanachchi,

Department of Physics and Center of Integrated Functional Materials, University of South Florida, Tampa, FL 33620

### ABSTRACT

We report evidence of enhancement in ferroelectricity in thin films of vanadium (V) doped ZnO grown at higher oxygen pressure. This process reduces oxygen deficiency and the material becomes very insulating, which in turn lowers the leakage current through the ferroelectric capacitor. 2 at. % V doped ZnO films, with thickness of approximately 1  $\mu\text{m}$  were grown epitaxially on c-cut sapphire ( $\text{Al}_2\text{O}_3$ ) (0001) at a growth temperature of 600°C. X-ray analysis showed the layers to be epitaxial where the (0002) diffraction peak had a rocking curve FWHM below 1°. The films with higher oxygen pressure were more insulating than the one grown with lower oxygen pressure. The saturation polarization doubled when the growth pressure increased from 300 mT to 500 mT. Time gated ICCD imaging of the ablated plasma during various  $\text{O}_2$  pressures and how it translated to the film quality are presented.

### INTRODUCTION

Wide band gap semiconductor ZnO has sustained research interest for quite some time because of its multifunctionality like ferromagnetism [1], piezoelectricity [2], optoelectronic [3], gas sensing [4], photocatalysis [5] etc. In this work, we look at the piezoelectricity and spontaneous polarization properties of ZnO and how it can be affected by dopants and growth conditions. It has been found that ZnO has the strongest piezoelectric response among the tetrahedrally bonded semiconductors [6]. This property of ZnO makes it a suitable material for technological application that require strong electromechanical coupling such as sensors and actuators [7]. Recently, Yang et al. [8, 9] has reported an electromechanical  $d_{33}$  coefficient of V-doped ZnO to be as high as 110 pC/N. This value is an order higher compared to the  $d_{33}$  coefficient of bulk ZnO [10] which is 9.9 pC/N. Yang et. al. further show that the  $d_{33}$  coefficient has a maximum value for 2.5 at. % of V doping. The another significant property due to V doping is reported to be the switchable spontaneous electric polarization. A butterfly like displacement graph is reported as a signature of spontaneous polarization [8]. Doping divalent cation Zn sites by V ions creates a mixed valency as well as strain in the original ZnO hexagonal structure because of the reduced ionic size of vanadium. It is reported that the V ions which replace the Zn sites are in  $5^+$  valency state [9]. The mixed valency creates charge polarity between Zn-O and V-O bonds. This charge polarity and the rotation of the nonlinear V-O bonds w.r.t. Zn-O bonds under electric field gives enhanced ferroelectricity [8].

In addition to V-doping, we need to create highly insulating films to further improve ferroelectric properties by reducing the leakage current. For this, we need to suppress the intrinsic oxygen vacancies. It is well known that ZnO grows with intrinsic oxygen deficiency which in turn is believed to give ferromagnetism and high conductivity in this material. Therefore we have grown epitaxial V-doped ZnO film under different oxygen pressure from 100 mT to 500 mT using pulsed laser ablation. The films with higher oxygen pressure are more

insulating than the one grown with lower oxygen pressure. The saturation polarization is higher for the film grown at higher pressure.

## **EXPERIMENT**

Thin films of V doped ZnO were grown on c-cut sapphire ( $\text{Al}_2\text{O}_3$ ) (0001) substrates using pulsed laser ablation technique. For this a ceramic target  $\text{Zn}_{1-x}\text{V}_x\text{O}$  ( $x=0.02$ ) was first prepared by standard solid state reaction method. Highly pure (99.99%) powders of ZnO and  $\text{V}_2\text{O}_5$  were mixed in stoichiometric proportion and well ground before being calcined in air for 6 hrs at  $600^\circ\text{C}$ . The calcined mixture was ground again and cold pressed under a pressure of 90 MPa into a one inch diameter and a quarter inch thick target. The pressed target was sintered at  $1000^\circ\text{C}$  in air for 12 hrs. A KrF excimer laser of wavelength 248 nm was used to ablate the compressed target. The chamber was pumped to a base pressure of  $4 \times 10^{-6}$  Torr and the films were grown at a pressure of 100 mT to 500 mTorr of oxygen while heating the substrate to  $600^\circ\text{C}$ . The repetition rate of the laser pulse was kept at 10 Hz and the fluence at the target surface was chosen to be  $2\text{J}/\text{cm}^2$ . The distance between the substrate and the target was 4 cm. Under these growth conditions, the rate of growth was measured to be approximately  $0.1 \text{ \AA}/\text{pulse}$ . The film crystallinity and orientation were assessed by conventional  $\theta$ - $2\theta$  x-ray diffraction (XRD) methods. The polarization hysteresis measurements were performed using the Precision LC from Radiant Technologies, which implies Sawyer-Tower Circuit.

## **DISCUSSION**

The growth parameters were optimized by first studying the laser-target interaction. At the same time, the ablated plume profile was studied at various combinations of laser fluences and oxygen pressure. The following subsections give a detail account of laser-target interaction, characterization of the thin films grown and the observed electric polarization as a function of oxygen pressure during the growth.

### **Laser Target Interaction**

Laser pulses of varying fluences from  $1\text{J}/\text{cm}^2$  to  $5\text{J}/\text{cm}^2$  were impinged separately on the fresh target surfaces to study the target surface morphology and the stoichiometry by using energy dispersive spectroscopy (EDS). Figure 1 shows an SEM micrograph of the zinc oxide target surface before and after the laser ablation. The ablated region shows a melted surface with hexagonal facets characteristic of zinc oxide. To study how the Vanadium (V) content changes in the target, EDS was performed on V-doped ZnO target surface irradiated with laser fluences from  $1\text{J}/\text{cm}^2$  to  $5\text{J}/\text{cm}^2$ . The Vanadium content did not change with the fluence. The standard deviation for the Vanadium content (at. %) on the target after laser ablation was 0.21. However, for larger fluence, large particulates appeared to come out of the target surface leaving behind voids of micron sizes. Although Vanadium content remained same for all the fluences, the ablated target surface looked smoothest and almost void free as shown in figure 1 for low fluence ( $2\text{J}/\text{cm}^2$ ). Thus  $2\text{J}/\text{cm}^2$  fluence was fixed for the film growth and the thin films grown had smooth surface and better crystallinity.

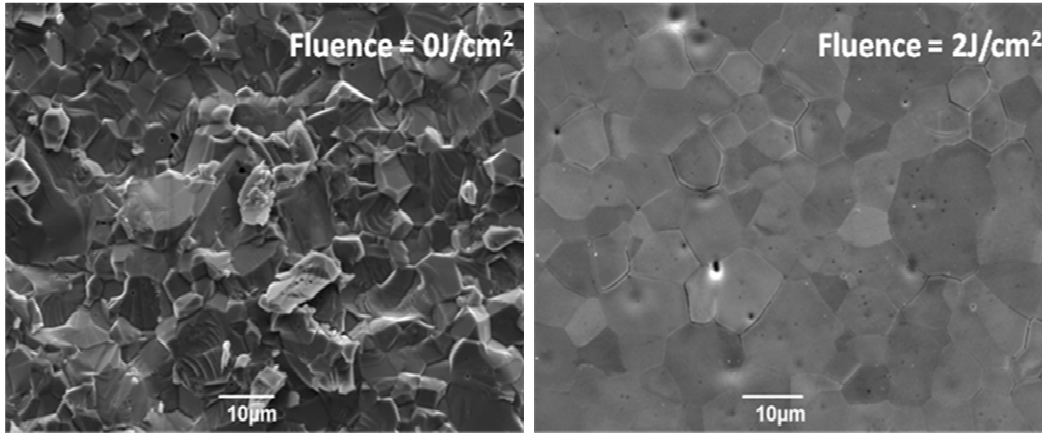


**Figure 1:** SEM pictures of unablated (left) and  $2\text{J}/\text{cm}^2$  ablated surface of ZnO ceramic target. 1000 laser pulses were used to ablate the target

### Thin film Growth

To reduce the oxygen deficiency and eventually to reduce leakage current through the ferroelectric capacitor we grew thin films with various oxygen pressures from 100 mT to 500 mT. Keeping the laser fluence at  $2\text{J}/\text{cm}^2$ , the laser ablated plumes were photographed by time gated Intensified Charge Coupled Detector (ICCD).

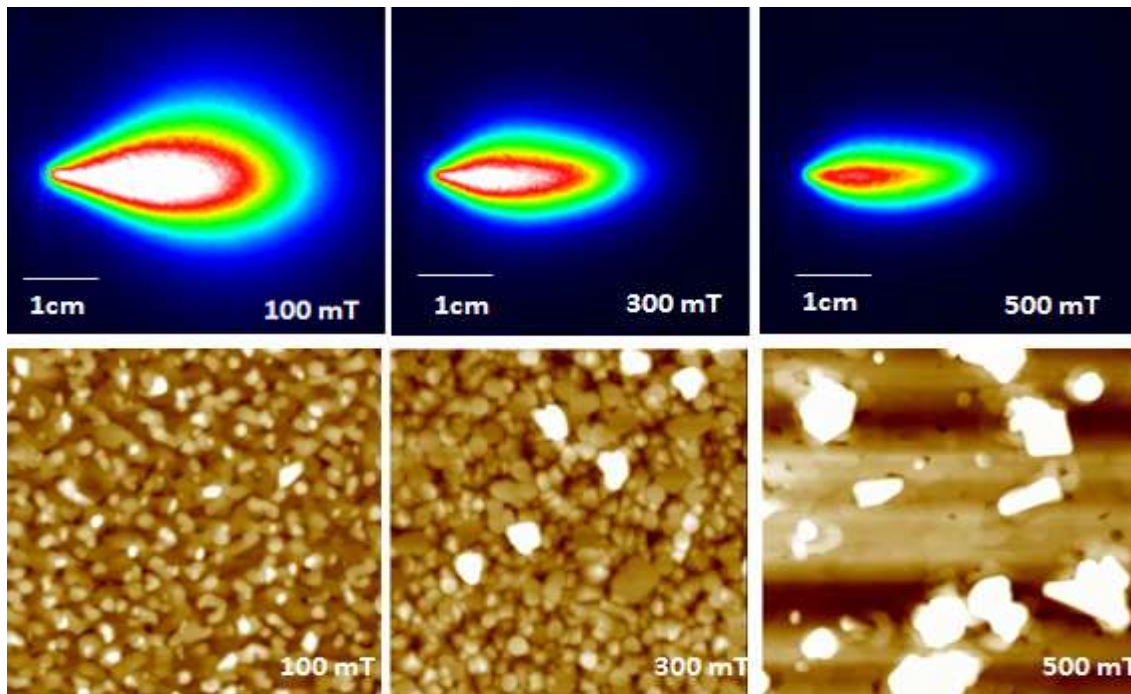


**Figure 2 :** Laser ablated plume images taken by ICCD for various oxygen pressures. 2 cm from the target, the FWHMs of the intensity lines for 100mT, 300mT and 500mT Oxygen ( $\text{O}_2$ ) pressure are 1.10 cm, 0.71 cm and 0.54 cm respectively. The lower panel shows the corresponding AFM images ( $5\mu\text{m} \times 5\mu\text{m}$ ) of the films grown on c-cut sapphire ( $\text{Al}_2\text{O}_3$ ) substrates.

The induced plasma images were taken for the duration of 20 $\mu$ s to capture the full expansion profile for all oxygen pressures from 100 mT to 500 mT. As shown in Fig.2, the plasma is more expanded for 100 mT oxygen pressure, but gets confined in forward direction as the oxygen pressure increases. Thin films of 2 at. % V-doped ZnO were grown at 100 mT, 300mT and 500mT on sapphire substrate heated at 600°C. As the growth pressure rises, more particles appear on the surface (Fig.2). For higher O<sub>2</sub>, the plasma plume is more directed and this tends to create nucleation sites on the film where the particles appear to grow faster. To make sure that the particles are not any foreign object, EDS was performed on top of the particles. The EDS showed spectra only from Zn and O confirming that the particles are no other than the ZnO crystals. Total emission intensity for 100 mT O<sub>2</sub> was the greatest indicating higher ionization concentration. Total emission intensity of 300 mT O<sub>2</sub> is 62% of 100mT O<sub>2</sub> and that of 500 mT O<sub>2</sub> is 45%. In addition the full width at half maximum of the plume intensity profile (FWHM) for 500mT of O<sub>2</sub> pressure is the lowest (0.54 cm) at 2 cm from the target which in turn leads to a lower deposition profile [11]. A roughness analysis was performed on these films. It is found that the root mean square roughness (Rq) for the films grown at 100mT, 300mT and 500mT was 17.5 nm, 33.5 nm and 55.8 nm, respectively. The Rq increased by three fold as the oxygen pressure increased from 100 mT to 500 mT.

To confirm the crystallinity and the epitaxy, X-ray diffraction measurements were done. Figure 3 shows the standard  $\theta$ -2 $\theta$  scan of the three films (grown at 100 mT, 300mT and 500mT) grown on c-cut sapphire (Al<sub>2</sub>O<sub>3</sub>) (0001) in which ZnO grows epitaxial along the (002) direction. All the films show (002) orientation. The rocking curves of the lattice-matched films are below 1 degree. However, FWHMs of the films grown at 300mT and 500mT are higher than the one grown at 100 mT (Fig.3).

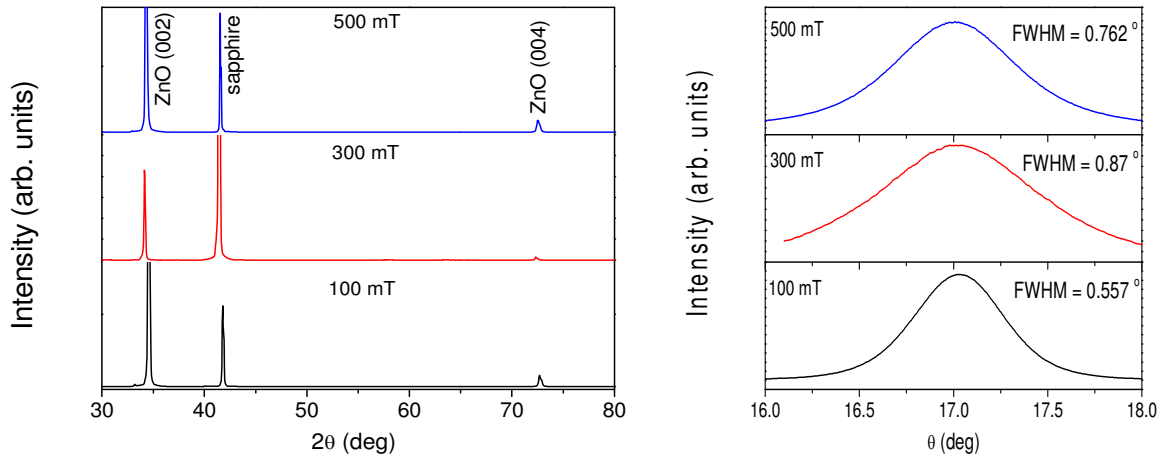


**Figure 3:** XRD peaks of 2 at. % V-doped ZnO grown on c-cut sapphire substrate. The right panel shows the rocking curves of (002) ZnO peak showing FWHMs.

### Electric Polarization

The resistivity and carrier concentrations were obtained by using Van der Pauw method. The films grown at higher O<sub>2</sub> pressure were more insulating and had less number of charge carriers. The results are summarized in Table 1. Since the film grown at 500mT was very insulating, it was not possible to obtain reliable data. As we can see from the table that the film

grown at 100 mT has low resistivity whereas the resistivity of the film grown at 300 mT is increased by five orders of magnitude. The electrical properties of a film grown at 200 mT is also included in Table 1 to show the trend in the films grown from 100 mT to 300 mT oxygen pressure. With the increase in resistivity of 300 mT film, the carrier concentration has reduced by about 4 orders of magnitude compared to the film grown at 100 mT of O<sub>2</sub> pressure.

**Table 1:** Resistivity and Hall measurement using Vander Paw Technique

Background Pressure (mT)	Sheet resistance R <sub>S</sub> (Ω)	Resistivity ρ(Ωcm)	Carrier Conc. n <sub>C</sub> (cm <sup>-3</sup> )	Mobility μ <sub>H</sub> (cm <sup>2</sup> /Vs)
100	2.76 × 10 <sup>2</sup>	8.82 × 10 <sup>-3</sup>	2.66 × 10 <sup>19</sup>	26.51
200	2.38 × 10 <sup>5</sup>	7.61	3.08 × 10 <sup>17</sup>	2.67
300	1.19 × 10 <sup>7</sup>	4.53 × 10 <sup>2</sup>	3.76 × 10 <sup>15</sup>	3.65

For electric polarization measurement, we fabricated a capacitor by depositing gold palladium electrodes on top of the film. Planar electrodes were used for both top and bottom electrodes because of the insulating substrate. Fig.4 shows the electric polarization for the three films. It can be seen that the polarization is the largest for the film grown at 500 mT. It is reported that V doped ZnO thin films show ferroelectricity due to the strain in the Zn-O bond where the Zn site is replaced by the smaller size V ion [8]. We further enhanced this polarization by growing the films at oxygen rich environment. With high oxygen pressure, we could grow films with less oxygen deficiency thus reducing the defects across the film. This reduced the leakage through the capacitor and we could measure the polarization at higher drive voltage.

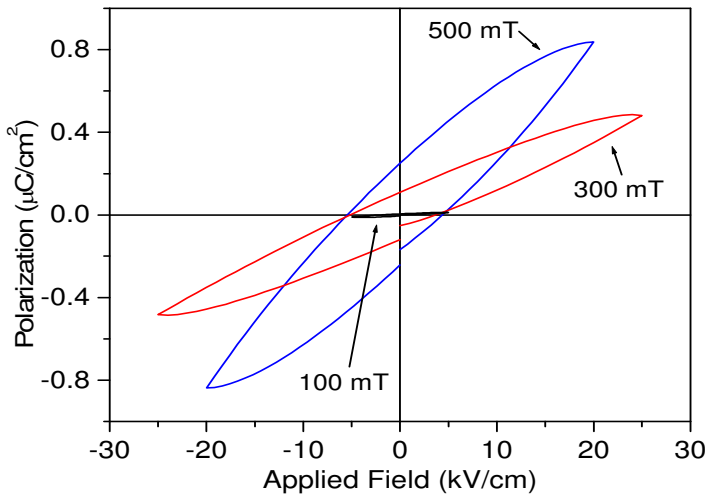


**Figure 4:** Electric Polarization as a function of applied electric field for the films grown at various oxygen pressures

The maximum value of saturation is approximately  $1\mu\text{C}/\text{cm}^2$  which is comparable to the published result [9]. Other parameters like the coercivities, remanent polarizations are summarized in Table 2 below.

**Table 2:** Saturation and remanent polarization and coercivities

Background Pressure (mT)	Saturation Polarization $P_S$ ( $\mu\text{C}/\text{cm}^2$ )	Remnant Polarization $P_R$ ( $\mu\text{C}/\text{cm}^2$ )	Coercive Field $E_C$ (kV/cm)
100	0.01	0.0045	2.05
300	0.48	0.1	4.4
500	0.83	0.24	4.9

## CONCLUSIONS

Ferroelectric switching was obtained in ZnO by doping it with penta-valent V ion. Higher saturation polarization was obtained for the film grown at higher oxygen pressure because of the more insulating nature of the film. The ICCD imaging of the plasma expansion showed broader expansion for low  $\text{O}_2$  pressure and narrower expansion for higher  $\text{O}_2$  pressure, which correlated well with the roughness of the film surface as obtained from AFM measurement.

## ACKNOWLEDGMENTS

This work was supported in part by the National Science Foundation under the grants DMI-0217939, DMI-0078917 and by the Department of Defense under the grant W81XWH-07-1-0708.

## REFERENCES

1. P. Sharma et. al., Nature Materials, **2**, 673 (2003)
2. Andrea Dal Corso, Michel Posternak, Raffaele, and Alfonso Baldereschi, Physical Review B, **50**, 10175 (1994)
3. R. D. Vispute et. al, Applied Physics Letter, **73**, 348 (1998)
4. Q. H. Li, T. Gao, Y. G. Wang, and T. H. Wang, APPLIED PHYSICS LETTERS **86**, 123117 (2005)
5. Mrinal Dutta and Durga Basak, Nanotechnology **20**, 475602 (2009)
6. A. D. Corso et. al, Phys. Rev. B **50**, 10715 (2004)
7. T. Shibata et. al, Sens. Actuators, A **102**, 106 (2002)
8. Y. C. Yang et al., Appl. Phys. Lett. **92**, 012907 (2008)
9. Y. C. Yang et al., Appl. Phys. Lett. **90**, 242903, (2007)
10. M. H. Zhao et. al, Nano Lett. **4**, 587 (2004)
11. Pritish Mukherjee, John B. Cuff, and Sarath Witanachchi, Applied Surface Science, **127-129**, 620 (1998)